Soliton formation in σ models

Manuel Fiolhais,[1] João da Providência,[1] Mitja Rosina,[2] and Célia A. de Sousa[1]
[1]*Departamento de Física, Universidade de Coimbra, P3000 Coimbra, Portugal*
[2]*J. Stefan Institute and Faculty of Mathematics and Physics, University of Ljubljana, Ljubljana, Slovenia*
(Received 14 May 1997)

The connection between the linear σ model and the Nambu–Jona-Lasinio model is investigated on the basis of a conventional Hartree-Fock approach. As a missing link, an intermediate model is used: a linear σ model with quarks (including the Dirac sea) but no ''Mexican hat.'' This model is particularly convenient to study the conditions for soliton formation and the stability of the soliton when the Dirac sea is included. [S0556-2813(97)04312-4]

PACS number(s): 24.85.+p, 12.39.−x

I. INTRODUCTION

In the past, considerable attention has been devoted to various σ models [1] in order to get a better understanding of the mechanism of chiral symmetry breaking in QCD. More recently, the Nambu–Jona-Lasinio (NJL) model [2] has gained prominence in this respect. The linear σ model is generally applied to valence quarks in order to describe the properties of low-lying states of the baryonic sector [3,4]. On the other hand, the NJL model is usually used to describe mesons that are seen as quark-antiquark $(q\overline{q})$ excitations of the chirally deformed vacuum [5,6]. Although widely studied in the literature, a deeper understanding of the σ model is lacking and this is the first motivation of our paper.

The linear σ model with quarks is often regarded as an approximation to the NJL model. The connection between both models has been discussed in the literature using the technique of path integration over collective fields [7]. We discuss the connection between both models on the basis of Hartree-Fock techniques. This framework, which is familiar to the nuclear physics community, provides in a very intuitive way the connection between the ''Mexican hat'' and the polarization of the Dirac sea of quarks. We try to establish the missing link between the linear σ model with ''Mexican hat'' and without sea quarks (we denote it as $\hat{\sigma}$ model), and the NJL model, in which the sea quarks play a crucial role. We show that the link is well described by an intermediate model: a linear σ model with the Dirac sea of quarks and without ''Mexican hat'' (we denote it as $\widetilde{\sigma}$ model). The mesonic self-interaction (the ''Mexican hat'') is replaced by the interaction of the Dirac sea with the classical σ and π fields. We regard the ''Mexican hat'' as a manifestation of the Dirac sea. Since the Dirac sea is included in the model, the ''Mexican hat'' is excluded in order to avoid double-counting.

The main motivation of our paper is, however, to study conditions for soliton formation. It is well known that the $\hat{\sigma}$ model with three valence quarks yields solitonic solutions for an appropriate range of the coupling constant [3,4,8,9]. For the NJL, the conditions for soliton formation are not yet well understood; in [10] the three-valence-quark soliton (nucleon) is obtained with the assumption that the auxiliary σ and π fields (which determine the valence single-particle quark states) lie on the chiral circle. The proposed intermediate model, the $\widetilde{\sigma}$ model, is very appropriate to study this question. We show that for a range of model parameters it gives a soliton and that the presence of the sea causes no instability in the model with a momentum cutoff.

Along the above lines this paper is organized as follows. In Sec. II we present the $\widetilde{\sigma}$ model and calculate the vacuum properties. In Sec. III we describe a soliton in the Thomas-Fermi approximation. The Thomas-Fermi approximation is valid for a large soliton (with many valence quarks, a ''quark star''), but some qualitative conclusions are instructive also for a nucleon. The soliton is also calculated in the NJL model in the framework of the Thomas-Fermi approximation. As expected, it is found that the obtained results in this context essentially coincide with, or are very similar to the results of the $\widetilde{\sigma}$ model. In Sec. IV we describe the pionic and sigma oscillations around the equilibrium vacuum value. We show that in the $\widetilde{\sigma}$ model important facts of PCAC and current algebra relations are preserved. In Sec. V we calculate the spherical three-valence-quark soliton by solving the Dirac equation for the s-state valence quarks in the self-consistent σ and π hedghog fields while still keeping the Thomas-Fermi approximation for the sea quarks.

II. THE $\widetilde{\sigma}$ MODEL AND QUARK MATTER

We consider a model of interacting quarks and mesons whose Hamiltonian may be written in the form

$$H_{\widetilde{\sigma}}=\sum_{k=1}^{N}\{\mathbf{p}_k\cdot\boldsymbol{\alpha}_k+g\beta_k[\Phi(\mathbf{r}_k)+i\gamma_{5k}\vec{\tau}_k\cdot\vec{\Psi}(\mathbf{r}_k)]+m_0\beta_k\}$$
$$+\frac{1}{2}\int \mathrm{d}^3\mathbf{r}[\Pi_\Phi^2+\vec{\Pi}_\Psi^2+\boldsymbol{\nabla}\Phi\cdot\boldsymbol{\nabla}\Phi+\boldsymbol{\nabla}\Psi_\alpha\cdot\boldsymbol{\nabla}\Psi_\alpha$$
$$+m^2(\Phi^2+\vec{\Psi}^2)], \tag{1}$$

where $\boldsymbol{\alpha}_k,\beta_k,\gamma_{5k}$ stand for the standard Dirac matrices acting on the degrees of freedom of the particle k; $\vec{\tau}_k$ stands for the corresponding isospin matrices; Φ and $\vec{\Psi}$ are, respectively, the (scalar-isoscalar) sigma and the (pseudoscalar-isovector) pion fields; $\Pi_\Phi,\vec{\Pi}_\Psi$ are the corresponding conju-

gate momenta. The total number of quarks in positive and negative energy states is N. The interaction term (the term starting with g) implies a momentum cutoff Λ for quarks; such momentum cutoff is not just a method to regularize the theory but it rather incorporates the finite size of quarks and/or mesons. Since the quark states with momenta beyond the cutoff do not interact they can be ignored. We emphasize that the cutoff has been introduced in the Hamiltonian, but this allows to look for the solutions in the truncated Fock space constructed from quark single-particle states with momenta smaller than Λ. The truncated Hilbert space should be invariant under the relevant symmetry group of the model, namely, the group of chiral rotations. Therefore the same truncation (momenta smaller than Λ) must be used for negative energy states and positive energy states.

The model parameters are g, Λ, m and the current quark mass m_0. We consider the chiral limit $m_0=0$ except when dealing with pion properties (Sec. IV).

The vacuum is described by constant meson fields and by a Slater determinant $|\Phi_0\rangle$, constructed out of plane waves which are negative energy eigenfunctions of the single particle hamiltonian $h=\mathbf{p}\cdot\boldsymbol{\alpha}+\beta M$. The ''constituent mass'' M of the particles is treated as a variational parameter.

The homogeneous quark matter is also described by a Slater determinant which now includes positive energy eigenstates of h up to the Fermi momentum p_F.

The density matrix for the homogeneous quark matter, which is diagonal in the $\mathbf{p}$ index but not in Dirac indices, is given by

$$\rho=\frac{1}{2}\left(1-\frac{\mathbf{p}\cdot\boldsymbol{\alpha}+\beta M}{\sqrt{p^2+M^2}}\right)\theta(\Lambda^2-p^2)+\frac{1}{2}\left(1+\frac{\mathbf{p}\cdot\boldsymbol{\alpha}+\beta M}{\sqrt{p^2+M^2}}\right)\theta(p_F^2-p^2). \tag{2}$$

For a state of equilibrium, the momenta $\Pi_\Phi,\vec{\Pi}_\Psi$ vanish and the fields $\Phi,\vec{\Psi}$ are also constant in time. Moreover, for the present choice of single particle states, $\vec{\Psi}=0$. The energy expectation value is

$$\mathcal{E}=\langle\Phi_0|H|\Phi_0\rangle=-\frac{\mathcal{N}V}{(2\pi)^3}\int_{(\Lambda>|\mathbf{p}|>p_F)}\mathrm{d}^3\mathbf{p}\frac{p^2+g\Phi M}{\sqrt{p^2+M^2}}+\frac{1}{2}m^2\Phi^2V, \tag{3}$$

where V denotes the normalization volume and the degeneracy due to spin, flavor and color is $\mathcal{N}=\mathcal{N}_s\mathcal{N}_f\mathcal{N}_c=12$.

Variation of the energy with respect to M leads to

$$\frac{\partial\mathcal{E}}{\partial M}=\mathcal{N}V(M-g\Phi)\int_{p_F}^{\Lambda}\frac{p^2\mathrm{d}p}{2\pi^2}\frac{p^2}{(p^2+M^2)^{3/2}}=0, \tag{4}$$

which is satisfied for

$$M=g\Phi. \tag{5}$$

The variation of $\mathcal{E}$ with respect to Φ yields

$$\frac{\partial\mathcal{E}}{\partial\Phi}=m^2\Phi V-\mathcal{N}gMV\int_{p_F}^{\Lambda}\frac{p^2\mathrm{d}p}{2\pi^2}\frac{1}{\sqrt{p^2+M^2}}=0. \tag{6}$$

Inserting (5) into this equation one concludes that (6) is trivially fulfilled for $M=0$ (hence $\Phi=0$). For $M=0$ the following self-consistency condition for hadronic matter with Fermi momentum p_F is obtained:

$$m^2=\mathcal{N}g^2\int_{p_F}^{\Lambda}\frac{p^2\mathrm{d}p}{2\pi^2}\frac{1}{\sqrt{p^2+M^2}}. \tag{7}$$

This is the so-called gap equation. Hereafter we denote by $M=M_{p_F}$ the solution of this equation and by $M=M_0$ the corresponding solution for $p_F=0$.

Inserting (5) back into the energy (3) one gets

$$\mathcal{E}=-\mathcal{N}V[F(\Lambda,M_{p_F})-F(p_F,M_{p_F})]+\frac{m^2M_{p_F}^2V}{2g^2}, \tag{8}$$

where

$$F(X,M)=\int_0^X\frac{p^2\mathrm{d}p}{2\pi^2}\sqrt{p^2+M^2}. \tag{9}$$

A seemingly more general ansatz corresponds to using the eigenfunctions of the Hamiltonian $h=p\cdot\boldsymbol{\alpha}+\beta M+i\beta\gamma_5\vec{\tau}\cdot\vec{M}_\Psi$ to construct the Slater determinant $|\Phi_0\rangle$ and treat M and $\vec{M}_\Psi$ variationally. The density matrix can be obtained by chirally rotating the form (2) and it leads to exactly the same minimal energy for any M and $\vec{M}_\Psi$ whose combination $\mathcal{M}=\sqrt{M^2+\vec{M}_\Psi^2}$ is the same. Therefore we are free to chose from degenerate ground states the one with vanishing $\vec{M}_\Psi$ and pion field.

As the order parameter related with the spontaneously broken chiral symmetry we introduce the ''quark condensate''

$$Q=\langle\overline{\psi\psi}\rangle=\langle\overline{\psi_u}\psi_u\rangle+\langle\overline{\psi_d}\psi_d\rangle=\frac{\mathrm{Tr}\rho\beta}{V}=-\mathcal{N}\int_{p_F}^{\Lambda}\frac{p^2\mathrm{d}p}{2\pi^2}\frac{M}{\sqrt{p^2+M^2}}=-\left(\frac{m}{g}\right)^2M. \tag{10}$$

The following comments are in order.

(i) The parameter g has no influence on the properties of the model except through the combinations $M=g\Phi_v$ and $(m/g)^2$. We do not need it here if we use as model parameter $(m/g)^2$ and if we are not interested in the unobservable vacuum expectation value of sigma, Φ_v.

(ii) m is not the mass of the sigma meson and does not have a direct physical meaning. Therefore we prefer to use M as input parameter and determine m/g from the gap equation (7). We interpret M as the constituent quark mass and choose it phenomenologically in the range 0.30–0.45 GeV.

(iii) The regime of the results depends only on the dimensionless ratio Λ/M and M only determines the energy (or length) scale. The ratio Λ/M can be determined from Eq. (10) using as input the phenomenological order parameter

$Q \approx -(0.283\ \mathrm{GeV})^3$. For typical constituent quark masses it follows a rather low cutoff value $\Lambda/M = 1.80$.

III. THE SOLITON WITH VALENCE QUARKS AND DIRAC SEA

We analyze now, from a variational point of view, the possibility of having N_+ quarks in positive energy states localized in a certain domain D or, in other words, whether it is energetically favorable for a soliton to be formed in the $\tilde{\sigma}$ model. We describe the single particle states by plane waves, now with an r-dependent mass, which is a good approximation for a system with many particles. In addition we chose the chiral angle such that $\vec{\Psi} = 0$ and therefore the fermion mass just comes from the sigma meson. The energy functional for the system with $\boldsymbol{r}$-dependent mass reads

$$\mathcal{E}[M] = \int \mathrm{d}^3\mathbf{r}\left[\mathcal{N}F(p_F(\mathbf{r}),M(\mathbf{r})) - \mathcal{N}F(\Lambda,M(\mathbf{r})) + \frac{m^2M^2(\mathbf{r})}{2g^2} + \frac{1}{2g^2}\boldsymbol{\nabla}M\cdot\boldsymbol{\nabla}M\right]. \tag{11}$$

Integration is throughout space and a gradient term which does not appear in (8) should be noticed. The Fermi-momentum is $\mathbf{r}$-dependent and is given by $p_F(\mathbf{r}) = \sqrt{\epsilon_F^2 - M^2(\mathbf{r})}$ if $\epsilon_F^2 - M^2(\mathbf{r}) > 0$ and $p_F(\mathbf{r}) = 0$ if $\epsilon_F^2 - M^2(\mathbf{r}) < 0$, in the spirit of the Thomas-Fermi method. However, the regularization cutoff Λ does not depend on r. According to the Thomas-Fermi method the following constraint:

$$\int \mathrm{d}^3\mathbf{r}\frac{\mathcal{N}p_F^3(\mathbf{r})}{6\pi^2} = N_+, \tag{12}$$

which fixes the particle number, must be imposed in the variational principle for the energy. Since the normalization volume is kept constant, the corresponding vacuum energy also remains unchanged, so it is legitimate to subtract it. This procedure is not an *ad hoc* rule but a logical consequence of our model. If it is followed, the energy functional of the soliton becomes

$$\mathcal{E}_{\mathrm{sol}}[M] = \int_D \mathrm{d}^3\mathbf{r}\left[\mathcal{N}F(p_F(\mathbf{r}),M(\mathbf{r})) - \mathcal{N}F(\Lambda,M(\mathbf{r})) + \frac{m^2M^2(\mathbf{r})}{2g^2} - \left(-\mathcal{N}F(\Lambda,M_0) + \frac{m^2M_0^2}{2g^2}\right) + \frac{1}{2g^2}\boldsymbol{\nabla}M\cdot\boldsymbol{\nabla}M\right], \tag{13}$$

where D is the domain where $M^2(\mathbf{r}) \neq M_0^2$.

So far we did not discuss the conditions for the soliton formation which we do now. For the sake of simplicity we shall consider a domain D, with volume x. Inside this volume the Fermi momentum p_F is constant and, therefore, the quarks have a constant mass M_{p_F}, whereas their mass outside the soliton is M_0. From (12) one gets the relation between the volume and the Fermi momentum for a certain number of particles in positive energy states:

$$\frac{6\pi^2N_+}{\mathcal{N}p_F^3} = x. \tag{14}$$

The energy of the system is

$$\mathcal{E} = x\left[\mathcal{N}F(p_F,M_{p_F}) - \mathcal{N}F(\Lambda,M_{p_F}) + \frac{m^2M_{p_F}^2}{2g^2}\right] + (V-x)\left[-\mathcal{N}F(\Lambda,M_0) + \frac{m^2M_0^2}{2g^2}\right], \tag{15}$$

where the last term represents the vacuum contribution from the region outside the soliton. For a given number of positive energy quarks, the equilibrium volume is determined by minimizing this expression with respect to x. For a set of parameters M_0, Λ and p_F the quark mass inside the soliton is the solution of the equation

$$\int_0^\Lambda \frac{p^2\mathrm{d}p}{\sqrt{p^2+M_0^2}} = \int_{p_F}^\Lambda \frac{p^2\mathrm{d}p}{\sqrt{p^2+M_{p_F}^2}}, \tag{16}$$

for p_F below the critical value for which chiral symmetry restoration occurs. Beyond that value, $M_{p_F} = 0$.

It is interesting to plot, as a function of the Fermi momentum (or as a function of the density N_+/x), the soliton energy per positive energy particle

$$\frac{\mathcal{E}_{\mathrm{sol}}}{N_+} = \frac{6\pi^2}{p_F^3}\left[F(p_F,M_{p_F}) - F(\Lambda,M_{p_F}) + F(\Lambda,M_0) + \frac{m^2}{2g^2\mathcal{N}}(M_{p_F}^2 - M_0^2)\right]. \tag{17}$$

In Fig. 1, this quantity, subtracted by the free quark mass M_0, is plotted as a function of the Fermi momentum for three sets of the model parameters. It is interesting to note that the transition between the regime of stable to the regime or metastable solitons occurs at the value $\Lambda/M = 1.80$ which is very close to the physically relevant value mentioned in Sec. II. Whether this is a coincidence, or a feature of the soliton formation remains an open question.

It is interesting to estimate the ratio between the number of active (i.e., below the cutoff Λ) Dirac sea quarks and the number of valence quarks in the soliton,

$$\frac{N_-}{N_+} = \left(\frac{\Lambda}{p_F}\right)^3 \approx 5.4, \tag{18}$$

for the equilibrium value of $p_F \approx 0.4$ GeV.

In Sec. V we shall treat the soliton with an $\mathbf{r}$-dependent quark mass, considering three valence quarks, now described quantically, while still keeping the semiclassical description of the Dirac sea.

In the present soliton we are not considering the gradient terms in (11). Therefore, in the framework of the time-

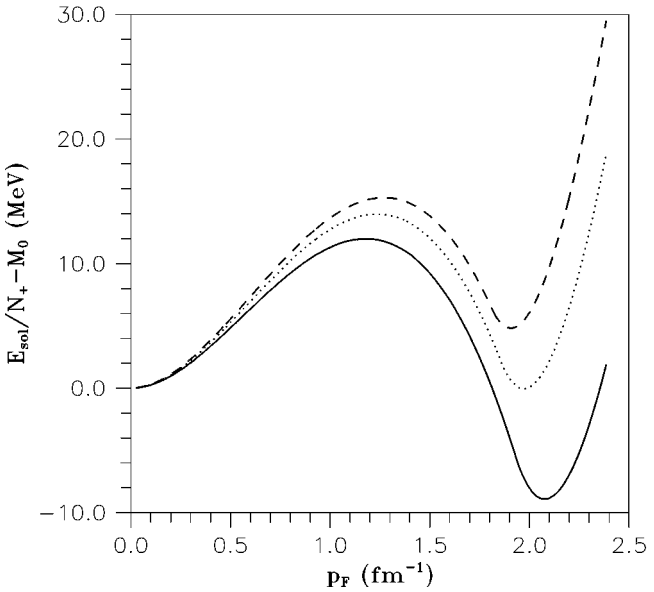

FIG. 1. Soliton energy per positive energy particle, subtracted by the free quark mass M_0 as a function of the Fermi momentum. The different curves correspond to $\Lambda/M_0=1.89$ (dashed line), $\Lambda/M_0=1.80$ (dotted line), and $\Lambda/M_0=1.67$ (solid line). We have used $\Lambda=0.7$ GeV.

independent mean field approximation, where $\Pi_\Phi=0$ and $\vec{\Pi}_\Psi=0$, the model (1) reduces to the so-called bosonized NJL. Note that the bosonized NJL is completely equivalent to the original NJL; it introduces the Φ and $\vec{\Psi}$ fields as auxiliary fields and not as new dynamical degrees of freedom as in the $\tilde{\sigma}$ model.

Moreover, the $\tilde{\sigma}$ model and the NJL model are equivalent as far as static properties are concerned. Thus, the results of interest so far obtained also apply to the NJL model. This remark is not valid, however, for the discussion in the next section, since the $\tilde{\sigma}$ model and the NJL model have similar but not identical dynamical properties.

We summarize now the NJL model. The Hamiltonian of this model may be written

$$H_{\rm NJL}=\sum_{k=1}^{N}\mathbf{p}_k\cdot\boldsymbol{\alpha}_k-\frac{g'}{2}\sum_{k,l=1}^{N}\delta(\mathbf{r}_k-\mathbf{r}_l)\times\beta_k\beta_l(1-\gamma_{5k}\gamma_{5l}\vec{\tau}_k\cdot\vec{\tau}_l). \tag{19}$$

The energy expectation value in the Hartree approximation is

$$\mathcal{E}=\langle\Phi_0|H|\Phi_0\rangle=-\frac{\mathcal{N}V}{2\pi^2}\int_{p_F}^{\Lambda}dp\,\frac{p^4}{\sqrt{p^2+M^2}}-\frac{g'}{2}V\left(\frac{\mathcal{N}}{2\pi^2}\int_{p_F}^{\Lambda}dp\frac{Mp^2}{\sqrt{p^2+M^2}}\right)^2. \tag{20}$$

Using Eq. (9) and the self-consistency condition for hadronic matter with Fermi momentum p_F,

$$1=\frac{\mathcal{N}g'}{2\pi^2}\int_{p_F}^{\Lambda}\frac{dpp^2}{\sqrt{p^2+M^2}}, \tag{21}$$

one gets, for the NJL model,

$$\mathcal{E}=-\mathcal{N}V[F(\Lambda,M_{p_F})-F(p_F,M_{p_F})]+\frac{M_{p_F}^2V}{2g'}. \tag{22}$$

The comparison between Eqs. (8) and (22) [or between (7) and (21)] establishes the equivalence between the $\tilde{\sigma}$ model and the NJL model with respect to *static properties*. Clearly, if the coupling constant in the NJL is chosen such that $g'=g^2/m^2$ the NJL and $\tilde{\sigma}$ model results are the same, namely the curves shown in Fig. 1. Finally, we note that if exchange terms are included, the factor g' in the self-consistency equation (21) changes to $g'(\mathcal{N}+1)/\mathcal{N}$.

For the $\hat{\sigma}$ model, whose mesonic potential (in the limit of chiral symmetry) reads

$$\mathcal{U}_{\hat{\sigma}}=\frac{\lambda}{4}(\Phi^2+\vec{\Psi}^2-\Phi_v^2)^2, \tag{23}$$

the soliton energy per positive energy particle is

$$\frac{\mathcal{E}_{\rm sol}}{N_+}=\frac{6\pi^2}{p_F^3}\left[F(p_F,M_{p_F})+\frac{\lambda}{4g^4\mathcal{N}}(M_{p_F}^2-M_0^2)^2\right], \tag{24}$$

where M_{p_F} is the solution of the self-consistency condition

$$\frac{\lambda}{g^4}(M_{p_F}^2-M_0^2)=-\frac{\mathcal{N}}{2\pi^2}\int_0^{p_F}\frac{p^2dp}{\sqrt{p^2+M_{p_F}^2}}. \tag{25}$$

The behavior of $\mathcal{E}_{\rm sol}/N_+$ [Eq. (24)] as a function of the Fermi momentum is similar to the behavior found in the $\tilde{\sigma}$ model (which is shown in Fig. 1). In particular, the shape depends only on the ratio λ/g^4 and M_0 just sets the scale. Similarly to Fig. 1 there are stable and metastable solitons. In Fig. 2 we compare $(\mathcal{E}_{\rm sol}/N_+)-M_0$ in the $\tilde{\sigma}$ model and in the $\hat{\sigma}$ model for stable solitons. In order to establish a comparison of the results the parameters in the $\tilde{\sigma}$ model are chosen to yield an effective meson potential with the minima located at the same position and with the same curvature at the minimum, in the sigma direction, as in the $\hat{\sigma}$ model (i.e., the sigma mass is the same in both models). From Fig. 2 one sees that the $\hat{\sigma}$ model soliton is more bound than the $\tilde{\sigma}$ model (or NJL), for corresponding model parameters. However, the minima occur at similar densities and, in both cases, already in the chiral symmetry restored phase. Another important difference between the the $\tilde{\sigma}$ model and the $\hat{\sigma}$ model is that in the $\tilde{\sigma}$ model the restoration of chiral symmetry is associated with a second order phase transition while in the $\hat{\sigma}$ model the phase transition is of first order. In other words, the quark mass M_{p_F} approaches 0 continuously in the $\tilde{\sigma}$ model and jumps discontinuously to 0 in the $\hat{\sigma}$ model, when

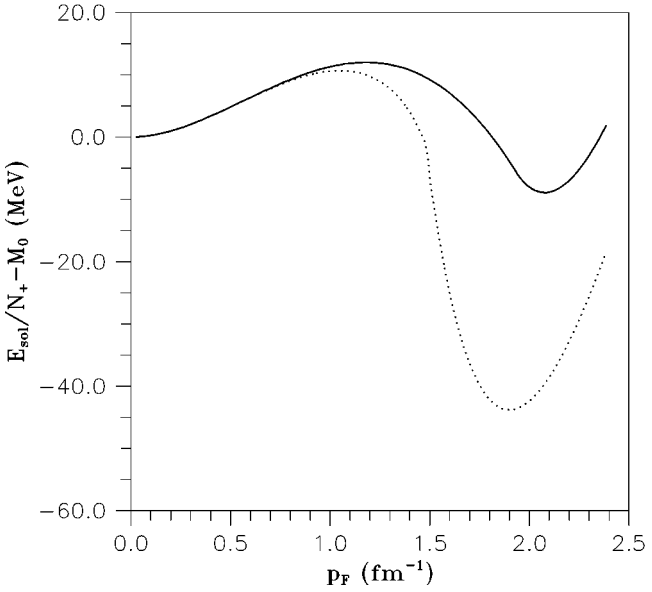

FIG. 2. Soliton energy per positive energy particle, subtracted by the free quark mass M_0 as a function of the Fermi momentum. The different curves correspond to the $\tilde{\sigma}$ model (solid line), and to the $\hat{\sigma}$ model (dashed line). The model parameters are $M_0=418.5$ MeV in both models and $\Lambda/M_0=1.67$ in the $\tilde{\sigma}$ model and $\lambda/g^4=0.13$ in the $\hat{\sigma}$ model. The solid line also corresponds to the NJL model which in this case is equivalent to the $\tilde{\sigma}$ model.

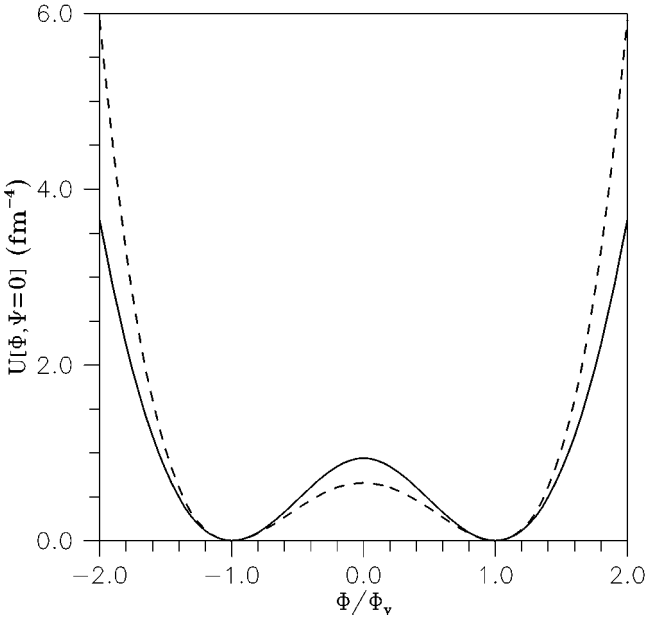

FIG. 3. Comparison between the mesonic self energy in the $\hat{\sigma}$ model (dotted line) and the Dirac-sea plus mesonic energy in the $\tilde{\sigma}$ model (solid line). The model parameters are indicated in the caption of Fig. 2.

chiral symmetry is restored as a result of an increase of p_F. The equivalence between the $\hat{\sigma}$ model and the NJL model is only qualitative.

IV. THE σ AND π EXCITATIONS

In the $\tilde{\sigma}$ model, the vacuum energy, in terms of the classical fields Φ and $\vec{\Psi}$, can then be written

$$\mathcal{E}=-\mathcal{N}V\int_0^\Lambda \frac{p^2 dp}{2\pi^2}\sqrt{p^2+g^2(\Phi^2+\vec{\Psi}^2)}+\frac{1}{2}m^2V(\Phi^2+\vec{\Psi}^2). \tag{26}$$

The behavior of the ground state energy (26), as a function of the fields Φ and $\vec{\Psi}$, resembles the ''Mexican hat'' potential (23).

In fact, the first term of Eq. (26) (quark sea energy) decreases quadratically for small Φ and, subsequently, for large Φ, decreases linearly. The second term, the mesonic potential energy, is positive quadratic throughout and dominates at large Φ. If the spontaneous symmetry breaking condition is satisfied, this positive second term is weaker than the negative first term near $\Phi=0$. So the energy $\mathcal{E}$ goes first quadratically down and then quadratically up. The ''Mexican hat'' (23), which represents the energy density of the vacuum, behaves very similarly, except that it raises quartically for very large Φ. Figure 3 shows the potentials for the $\tilde{\sigma}$ model and for the $\hat{\sigma}$ model (we set $\vec{\Psi}=0$) for the parameters used in Fig. 2. Since the parameters are chosen in order to have the same curvature around the minima, the agreement is particularly good there, where it is physically most interesting for excitations and for the hedgehog soliton (Sec. V). For the soliton studied in Sec. III the relevant region is in the range $0\leqslant\Phi\leqslant\Phi_v$ and the difference at $\Phi=0$ is responsible for the different binding energies of the $\tilde{\sigma}$ and $\hat{\sigma}$ solitons found in the previous section (see Fig. 2).

Expanding the right-hand side (RHS) of Eq. (26) around the equilibrium values $\Phi=\Phi_v$, $\vec{\Psi}=0$, expressions for the masses of the phenomenological structureless pion and sigma mesons are obtained,

$$m_\pi^2=\frac{1}{V}\frac{\partial^2\mathcal{E}}{\partial\vec{\Psi}^2}\bigg|_{(\Phi,\vec{\Psi})=(\Phi_v,0)}=m^2-\frac{\mathcal{N}g^2}{2\pi^2}\int_0^\Lambda\frac{dpp^2}{\sqrt{p^2+M^2}}=0, \tag{27}$$

$$m_\sigma^2=\frac{1}{V}\frac{\partial^2\mathcal{E}}{\partial\Phi^2}\bigg|_{(\Phi,\vec{\Psi})=(\Phi_v,0)}=m^2-\frac{\mathcal{N}g^2}{2\pi^2}\int_0^\Lambda\frac{dpp^4}{(\sqrt{p^2+M^2})^3}. \tag{28}$$

The NJL model and the $\tilde{\sigma}$ model are almost equivalent but not quite since they lead to slightly different dynamics. The familiar relation from the NJL model

$$m_\sigma^2=4M^2, \tag{29}$$

does not hold in the $\tilde{\sigma}$ model. Actually, having in mind Eqs. (28) and (29) in the chiral limit ($m_\pi=0$), it follows that

$$\frac{\mathcal{N}g^2}{2\pi^2}\int_0^\Lambda\frac{dpp^2}{(\sqrt{p^2+M^2})^3}=4. \tag{30}$$

The effect of Eq. (30) would be to fix a value for Λ/M but this quantity is no longer free since its value is fixed by the criterium described in the previous section. However, re-

TABLE I. Mesonic properties in the context of the $\tilde{\sigma}$-model and in the quark NJL model. The asterisk denotes results, concerning the NJL in the harmonic order, taken from Ref. [11]. We also include in brackets some experimental or phenomenological values.

		$\tilde{\sigma}$ model	NJL model
Mod. param.	coupling	$g=3.6$	$g'=1.098\times10^{-5}$ MeV^{-2}*
	Λ [MeV]	610.5	631.0*
	m [MeV]	1045.7	
	m_0 [MeV]	5.8	5.5*
			(7.0±1.9)
Inputs	f_π [MeV]	93	93*
			(93)
	m_π [MeV]	138	138*
			(138)
	$\langle\overline{\psi}\psi\rangle^{1/3}$ [MeV]	302.6	310.7*
			(283.5±31)
	M [MeV]	335	335*
			(350)
Outputs	m_σ [MeV]	669.4	675.3*
	$g_{\pi q}$	3.6	3.5*
			(2.7-3.7)
	$g_{\sigma q}$	3.6	2.2*
	$g_{\sigma\pi\pi}$ [MeV]	2306.5	1385.6
	$\Gamma_{\sigma\pi\pi}$ [MeV]	432.1	154.9
	$g_{4\pi}$	6.2	5.7

markably enough, the results obtained for m_σ, for both models, are, nevertheless, very similar (see Table I).

We identify Φ_v with the pion decay constant f_π as the Goldberger-Treiman (GT) relation $M=g\Phi_v$ suggests [see Eq. (5)]. In this context the parameter g has the physical meaning of the coupling constant between quarks and mesons.

By endowing the quarks with a small current mass m_0, chiral symmetry is explicitly broken and PCAC is achieved. Then, m_π no longer vanishes. Instead we obtain

$$m_\pi^2 f_\pi^2 \simeq -m_0\langle\overline{\psi}\psi\rangle, \tag{31}$$

which shows that the well known Gell-Mann-Oakes-Renner (GMOR) relation is verified in this simple model.

The parameters of the model can be fitted in order to obtain $f_\pi=93$ MeV, $m_\pi=138$ MeV as is shown in Table I.

In spite of the simplicity of this model with structureless mesons, the results obtained are in agreement with the general requirements of chiral symmetry.

From Eq. (26) we also obtain the meson coupling constants

$$g_{\sigma\pi\pi}=\frac{1}{2V}\frac{\partial^3\mathcal{E}}{\partial\Phi\,\partial\vec{\Psi}^2}\bigg|_{(\Phi,\vec{\Psi})=(\Phi_v,0)}=\frac{m_\sigma^2-m_\pi^2}{2f_\pi}, \tag{32}$$

$$g_{4\pi}=\frac{1}{24V}\frac{\partial^4\mathcal{E}}{\partial\vec{\Psi}^4}\bigg|_{(\Phi,\vec{\Psi})=(\Phi_v,0)}=\frac{m_\sigma^2-m_\pi^2}{8f_\pi^2}, \tag{33}$$

which, in the chiral limit, are related by the equation $g_{4\pi}=g_{\sigma\pi\pi}^2/(2m_\sigma^2)$.

The potential energy density of the effective boson Hamiltonian derived from the $\tilde{\sigma}$ model, taking into account dynamical as well as explicit breaking of chiral symmetry, can be written

$$\mathcal{U}=\frac{1}{2}m_\pi^2\vec{\Psi}^2+\frac{1}{2}m_\sigma^2\tilde{\Phi}^2+g_{\sigma\pi\pi}\tilde{\Phi}\vec{\Psi}^2+g_{4\pi}\vec{\Psi}^4+\cdots, \tag{34}$$

where $\tilde{\Phi}=\Phi-\Phi_v$.

Using the Fermi golden rule, the transition amplitude for the decay $\sigma\rightarrow\pi\pi$ is

$$\Gamma_{\sigma\pi\pi}=\frac{3g_{\sigma\pi\pi}^2}{16\pi m_\sigma}\left(1-\frac{4m_\pi^2}{m_\sigma^2}\right)^{1/2}. \tag{35}$$

The s-wave lengths of the $\pi\pi$ scattering are defined as usually and lead to results which agree with the Weinberg relation:

$$a_0^0=\frac{1}{32\pi}\left(\frac{7m_\pi^2}{f_\pi^2}\right), \tag{36}$$

$$a_0^2=\frac{1}{32\pi}\left(-2\frac{m_\pi^2}{f_\pi^2}\right). \tag{37}$$

V. THE HEDGEHOG SOLITON

The semiclassical (Thomas-Fermi) method considered in Sec. III to describe the quarks is certainly a good approximation if there are many negative and positive energy particles. However, if one is interested in the baryon structure, $N_+=3$ and a quantum description of the valence quarks is, obviously, necessary. On the other other hand, the number of sea-quarks should be big enough [see Eq. (18)] to allow for a semiclassical description which is used here.

We consider both the pion and the sigma fields which are assumed as classical fields in the spirit of a mean field approximation. The usual hedgehog form is used, namely

$$\Phi(\mathbf{r})=\Phi(r), \tag{38}$$

$$\vec{\Psi}(\mathbf{r})=\hat{\mathbf{r}}\varphi(r). \tag{39}$$

The $\mathcal{N}_c$ valence quarks occupy the lowest (nodeless) s state having the spin-isospin hedgehog structure:

$$|q_h\rangle=\frac{1}{\sqrt{4\pi}}\begin{pmatrix} u(r) \\ iv(r)\boldsymbol{\sigma}\cdot\hat{\mathbf{r}}\end{pmatrix}\frac{1}{\sqrt{2}}(|u\downarrow\rangle-|d\uparrow\rangle). \tag{40}$$

The radial functions $u(r),v(r),\Phi(r),\varphi(r)$ in (38)–(40) are determined variationally. The energy functional of the hedgehog (with the constant vacuum energy already subtracted) differs from (13) essentially in the quark valence contribution. The following variational equations are obtained, $M(r)=g\Phi(r)$ and $\vec{M}_\Psi(r)=g\vec{\Psi}(r)=g\hat{\mathbf{r}}\varphi(r)$, and the energy functional of the hedgehog in terms of the radial profiles $u(r),v(r),\Phi(r),\varphi(r)$, reads

$$\begin{aligned}\mathcal{E}[u,v,\Phi,\varphi]=\mathcal{N}_c\int_0^\infty\Big[&u\frac{\partial v}{\partial r}-v\frac{\partial u}{\partial r}+\frac{2uv}{r}+g\Phi(u^2-v^2)\\&+2g\varphi uv\Big]r^2\mathrm{d}r+2\pi\int_0^\infty\Big[\left(\frac{\partial\Phi}{\partial r}\right)^2+\left(\frac{\partial\varphi}{\partial r}\right)^2\\&+\frac{2\varphi^2}{r^2}\Big]r^2\mathrm{d}r+2\pi m^2\int_0^\infty[\Phi^2+\varphi^2-f_\pi^2]r^2\mathrm{d}r\\&-\frac{2\mathcal{N}}{\pi}\int_0^\infty r^2dr\int_0^\Lambda[\sqrt{p^2+(g\Phi)^2+(g\varphi)^2}\\&-\sqrt{p^2+(gf_\pi)^2}]p^2\mathrm{d}p,\end{aligned} \tag{41}$$

where we have already chosen the vacuum expectation value of the σ field, $\Phi_v=f_\pi$ and considered the chiral limit. The parameter m satisfies a self-consistency relation similar to (7):

$$m^2=\frac{\mathcal{N}g^2}{2\pi^2}\int_0^\Lambda\frac{p^2\mathrm{d}p}{\sqrt{p^2+(gf_\pi)^2}}. \tag{42}$$

We demand the energy functional (41) to be stationary with respect to variations of u, v, Φ, and φ subjected to the constraint

$$\int_0^\infty(u^2+v^2)r^2\mathrm{d}r=1. \tag{43}$$

This restriction is implemented in the variational principle by means of a Lagrange multiplier, ϵ (the valence quark eigenenergy). We recall that the cutoff parameter is independent of r. Therefore, contrary to the procedure followed in connection with quarks in positive energy states, whose number was fixed by (12), no constraint should be imposed to fix the number of sea-quarks. The variational principle leads to the following set of differential equations:

$$\frac{\partial u}{\partial r}=-(\epsilon+g\Phi)v+gu\phi, \tag{44}$$

$$\frac{\partial v}{\partial r}=-\frac{2v}{r}+(\epsilon-g\Phi)u-gv\phi, \tag{45}$$

$$\begin{aligned}\frac{\partial^2\Phi}{\partial r^2}=&-\frac{2}{r}\frac{\partial\Phi}{\partial r}+\frac{\mathcal{N}_cg}{4\pi}(u^2-v^2)+m^2\Phi\\&-\frac{\mathcal{N}g^2\Phi}{2\pi^2}\int_0^\Lambda\frac{p^2\mathrm{d}p}{\sqrt{p^2+(g\Phi)^2+(g\varphi)^2}},\end{aligned} \tag{46}$$

$$\begin{aligned}\frac{\partial^2\varphi}{\partial r^2}=&-\frac{2}{r}\frac{\partial\varphi}{\partial r}+\frac{2\varphi}{r}+\frac{\mathcal{N}_cg}{2\pi}uv+m^2\varphi\\&-\frac{\mathcal{N}g^2\varphi}{2\pi^2}\int_0^\Lambda\frac{p^2\mathrm{d}p}{\sqrt{p^2+(g\Phi)^2+(g\varphi)^2}}.\end{aligned} \tag{47}$$

These equations are similar to those obtained for the hedgehog in the $\hat{\sigma}$ model and they even reduce to the same asymptotic equations in the limit $r\to\infty$ [8]. It is therefore interesting to compare the two hedgehog solitons obtained in the $\widetilde{\sigma}$ model and in the $\hat{\sigma}$ model. In order to make the comparison we relate the model parameters as we already mentioned in Sec. III: f_π is fixed at the experimental value and we take the same coupling g in both models. For a given Λ in the $\widetilde{\sigma}$ model we use (28), which can be written in the form

$$m_\sigma^2=\mathcal{N}\frac{g^4f_\pi^2}{2\pi^2}\int_0^\Lambda\frac{p^2\mathrm{d}p}{(p^2+(gf_\pi)^2)^{3/2}}, \tag{48}$$

to compute the σ mass which is then used as input parameter in the $\hat{\sigma}$ model.

The radial functions of quarks $[u(r),v(r)]$ and mesons $[\Phi(r),\varphi(r)]$ are essentially the same in both models and this result is independent of the parameters. Qualitatively, the radial functions are very similar to those found in different model calculations in the literature [3,4,8,9], therefore we do not present them here.

In Fig. 4 we present the ratio between the *effective* sea-quark mass squared and the square of its mass in the vacuum $R=(\Phi^2+\varphi^2)/f_\pi^2$. Both solutions produce similar results with R in the range between ~1 and ~0.7. Such similarity is a consequence of the similarity of the potentials for the chiral mesons in that range as it can be recognized from Fig. 3. The similarity of both models is also corroborated by the results given in Table II for the quark eigenvalues and for the total soliton energy.

We note that the hedgehog soliton fields wind around the chiral valley, whereas in the soliton of Sec. III there were no

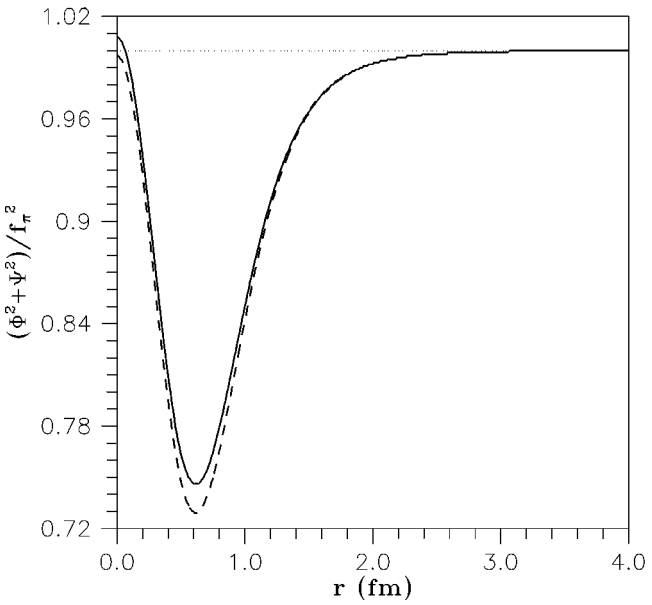

FIG. 4. Ratio of the square of the effective quark mass to the square vacuum quark mass for the hedgehog soliton in the $\tilde{\sigma}$ model and in the $\hat{\sigma}$ model. The model parameters are indicated in the caption of Fig. 2.

pions and the soliton sigma field interpolates between $\Phi=0$ at the center of the soliton and $\Phi=\Phi_v$ in the periphery. Therefore, the relevant region of the potential is quite different for the two solitons.

We remark that we have made an approximation, in solving Eqs. (45)–(47) since we have calculated the positive energy quark states in full space although we have introduced in the Hamiltonian [Eq. (1)] a momentum cutoff for both negative and positive energy states. We estimate that the error is small since we get admixtures of 8% (2%) of basic states with $p>\Lambda$ for the model parameters in the first (second) row of Table II. This result shows also that the question whether or not to truncate also positive-energy states is not very important, while the cutoff for negative energy states is essential for mathematics (to avoid divergencies) as well as for physics (finite size effect).

VI. CONCLUSION

We have shown that the linear $\tilde{\sigma}$ model with valence quarks and Dirac-sea quarks (but without the ''Mexican hat'') possesses the following features

(i) The interaction of the Dirac sea with the σ and π fields gives a similar energy contribution as the mesonic self-interaction (''Mexican hat'') in the conventional $\hat{\sigma}$ model. This energy contribution produces similar effects both for the soliton formation as well as for mesonic excitations of the vacuum.

TABLE II. Quark eigenvalues and soliton energies in GeV (Λ and m_σ also in GeV).

			$\tilde{\sigma}$ model		$\hat{\sigma}$ model	
g	Λ	m_σ	ϵ	$\mathcal{E}_{\rm sol}$	ϵ	$\mathcal{E}_{\rm sol}$
4.5	0.7	0.961	0.085	1.175	0.087	1.173
	0.9	1.140	0.079	1.186	0.080	1.185
5.0	0.7	1.094	0.019	1.089	0.021	1.089
	0.9	1.315	0.016	1.097	0.017	1.097

(ii) The proposed $\tilde{\sigma}$ model is also similar to the NJL model. In fact it differs from the bosonized version of NJL only by the additional gradient terms (implying that meson fields are not just auxiliary fields but represent new dynamical degrees of freedom).

The advantage of this $\tilde{\sigma}$ model over the conventional $\hat{\sigma}$ model is in a unified description of the baryonic sector (soliton) and the mesonic sector (chiral distortion of Dirac sea). The Dirac sea not only provides the effective mesonic self-interaction, but it contributes also to other physical quantities. For example, its contribution to the momentum is likely to give more realistic effects of linear momentum projection [12].

The advantage of the $\tilde{\sigma}$ model over the NJL model is that it is easier to handle. At first sight it seems the opposite since the $\tilde{\sigma}$ model contains the gradient terms in addition. But it turns out that they help to stabilize the calculation of the soliton with or without the chiral circle condition while in NJL the variational equations are ill-behaved if the chiral circle condition is not imposed in the variational procedure [10].

We believe that having two sets of degrees of freedom, $q\overline{q}$ and mesons, is not double counting since the full QCD is anyway very much richer than any of these models. The $\tilde{\sigma}$ model is just slightly richer than the NJL model. This does not change much the low-energy properties, but it improves some ambiguities in the calculation. It is a challenge to see whether at some important low energy properties really both degrees of freedom manifest themselves. We cannot give a definite answer yet but we conclude that the stabilizing effects in the soliton formation in the $\tilde{\sigma}$ model support this view.

ACKNOWLEDGMENTS

We are glad to acknowledge many critical remarks of Bojan Golli. This work was supported by the Ministry of Science and Technology of the Republic of Slovenia and by JNICT, Portugal (Contracts PRAXIS /2 /2.1 /Fis /451 /94, PRAXIS /PCEX /P /FIS /6 /96, and PESO /S /PRO /1057 /95).

[1] M. Gell-Mann and M. Levy, Nuovo Cimento **16**, 705 (1960).
[2] Y. Nambu and G. Jona-Lasinio, Phys. Rev. **122**, 345 (1961); **124**, 246 (1961).
[3] M. C. Birse and M. K. Banerjee, Phys. Lett. **136B**, 284 (1984).
[4] S. Kahana, G. Ripka, and V. Soni, Nucl. Phys. **A415**, 351 (1983).
[5] V. Bernard, R. Brockmann, M. Schaden, W. Weise, and E. Werner, Nucl. Phys. **A412**, 349 (1984).

[6] J. da Providência, M. C. Ruivo, and C. A. de Sousa, Phys. Rev. D **36**, 1882 (1987).
[7] E. R. Arriola, C. V. Christov, and K. Goeke, Phys. Lett. B **225**, 22 (1989).
[8] M. Fiolhais, K. Goeke, F. Grümmer, and J.N. Urbano, Nucl. Phys. **A481**, 727 (1988).
[9] B. Golli and R. Sraka, Phys. Lett. B **312**, 24 (1993); B. Golli and M. Rosina, *ibid.* **393**, 161 (1997).
[10] Chr. V. Christov, A. Blotz, H.-C. Kim, P. P. Pobylitsa, T. Watabe, Th. Meissner, E. Ruiz Arriola, and K. Goeke, Prog. Part. Nucl. Phys. **37**, 91 (1996).
[11] C. A. de Sousa, Z. Phys. C **43**, 503 (1989).
[12] T. Neuber and K. Goeke, Phys. Lett. B **281**, 202 (1992); A. Drago, M. Fiolhais, and U. Tambini, Nucl. Phys. **A609**, 488 (1996).